

Synthesis and Electrochemical Characterization of $\text{Li}_2\text{MnSiO}_4$ with Different Crystal Structure as Cathode Material in Lithium Rechargeable Batteries

Joongpyo Shim¹, Sora Won¹, Gyungse Park³, Ho-Jung Sun²

¹Department of Nano & Chemical Engineering, Kunsan National University, Gunsan, Jeonbuk, Korea

²Department of Material Science & Engineering, Kunsan National University, Gunsan, Jeonbuk, Korea

³Department of Chemistry, Kunsan National University, Gunsan, Jeonbuk, Korea

Email: jpsim@kunsan.ac.kr, hjsun@kunsan.ac.kr, parkg@kunsan.ac.kr

Received 2012

ABSTRACT

$\text{Li}_2\text{MnSiO}_4$ with different crystal structure was synthesized by solid state reaction method. Their crystal structure and electrochemical properties have been characterized by X-ray diffraction and charge-discharge test. The material prepared at 900°C in N_2 atmosphere had γ -phase and its crystal structure changed to β -phase by post-heating at 400°C in air after 900°C sintering. In electrochemical measurement, two materials (γ - and β -phase) showed ~3 and ~45mAh/g, respectively. The different capacities of these two materials might be due to the change of crystal structure.

Keywords: $\text{Li}_2\text{MnSiO}_4$; Crystal Structure; Cathode; Lithium Rechargeable Battery

1. Introduction

Recently, the lithium extraction/insertion in polyanion frame works, for example, $(\text{XO}_4)^n$ (X = P, S and Si) materials, has been shown by many researchers [1-3]. In particular, LiFePO_4 has been intensively studied as possible substitution for commercially available LiCoO_2 . But, its redox voltage and theoretical capacity have been limited to ~3.5V and 170mAh/g, respectively [4]. One of them, $\text{Li}_2\text{MnSiO}_4$, as cathode material in lithium rechargeable batteries provides very promising candidates to explore in place of LiCoO_2 because its high theoretical capacity of 333mAh/g. The Mn redox couple ($\text{Mn}^{2+}/\text{Mn}^{4+}$) is of particular interest due to a high potential (vs. Li/Li^+), plentiful resource and environmentally friendly material. Dominko et al. firstly found that only 0.6 Li^+ ions could be extracted at the first cycle, and 0.3 Li^+ could be reversibly extracted and inserted at 5th cycle at C/30 rate [5].

Politaev et al. reported the monoclinic $\text{Li}_2\text{MnSiO}_4$ was synthesized by high temperature sintering instead of orthorhombic structure by low temperature synthesis [6]. As explained by them and others [7], monoclinic $\text{Li}_2\text{MnSiO}_4$ is a superlattice of the high temperature orthorhombic $\text{Li}_{2(4b)}\text{Li}_{(2a)}\text{PO}_4$, where Mn^{2+} ions are located in the 2a tetrahedral sites within the $[\text{SiO}_4]^{4-}$ anionic silicate framework that replaces the $[\text{PO}_4]^{3-}$ anionic phosphate framework. Many studies showed that it was difficult to form pure orthorhombic $\text{Li}_2\text{MnSiO}_4$ from low temperature synthesis below 800°C [8,9].

There are few studies on two forms of $\text{Li}_2\text{MnSiO}_4$ on electrochemical characteristics. The aim of this work is to report the crystal structure change and the electrochemical properties of $\text{Li}_2\text{MnSiO}_4$ powders synthesized by different processes.

2. Experimental

$\text{Li}_2\text{MnSiO}_4$ was prepared using solid state reaction as following

process. Starting materials were lithium hydroxide (LiOH , Aldrich), manganese carbonate (MnCO_3 , Aldrich) and fumed silica (SiO_2 , Aldrich). Stoichiometric amounts of all precursors were weighed, grinded and mixed in mortar homogeneously. Thereafter, the product was dried at 100°C and then slowly heated to 900°C for 12h under nitrogen atmosphere to avoid the oxidation of Mn ion from Mn^{2+} to Mn^{3+} or Mn^{4+} by the reaction with oxygen [5]. Additional process, post heating at 400°C for 5h in air, was conducted to change crystal structure of $\text{Li}_2\text{MnSiO}_4$. Weight loss during heat-treatment was determined by thermal gravimetric analysis (TGA, TA Instrument).

The crystal structures of samples were identified by X-ray diffraction (XRD, PANalytical, EMPYREAN) in $\text{Cu K}\alpha$ radiation. The sample morphology and the chemical composition were analyzed by using a field emission scanning electron microscope (FE-SEM, FESEM, Hitachi, S-4800) with energy dispersive X-ray spectroscopy (EDS, Horiba, EX-250).

The electrode for electrochemical testing was prepared from 70 wt% $\text{Li}_2\text{MnSiO}_4$, 20 wt% carbon (Super-P) as conductive agent, and 10 wt% PVdF as binder. Firstly, all materials were mixed in NMP (1-methyl-2-pyrrolidone, Aldrich) for m. The \square 10h by ball-mill and then cast on an Al foil current collector (20 electrodes were dried at 120°C under vacuum to remove solvent and stored in an Ar-filled glovebox. Electrochemical measurements were carried out on CR 2032 coin cell (Hoshen) which was assembled in glovebox. The electrolyte was 1.0M LiPF_6 in a mixture (1:1:1) of ethylene carbonate (EC), ethyl methyl carbonate (EMC) and dimethyl carbonate (DMC) (Technosemichem). The coin cells were assembled with lithium foil (Aldrich) as negative electrode and polypropylene separator (Celgard). The charge & discharge tests were performed using a battery cycler (WBCS3000, WonAtech) in the voltage range of

2.0 – 4.7V (vs. Li/Li⁺) at room temperature.

3. Results and Discussion

TGA was carried out to observe the weight loss of precursors and the starting synthesis temperature, as shown in **Figure 1**. The mixture of precursors lost about 20% weight around 300°C, which was assigned to the evaporation of CO₂ and H₂O. And then, the weight of precursor decreased slowly until 700°C. Therefore, it assumes that the formation of Li₂MnSiO₄ starts above 700°C.

Figure 2 shows XRD patterns of Li₂MnSiO₄ sintered at 900°C in N₂ for 12h, and post-heated at 400°C in air for 5h after sintering. The XRD pattern of Li₂MnSiO₄ obtained after 900°C sintering indicates the formation of monoclinic (space group *P2₁/n*) structure (γ -phase). To get pure orthorhombic Li₂MnSiO₄ from monoclinic phase, post-heating process was conducted at 400°C in air for 5h. As shown in **Figure 1(b)**, disappearing the diffraction peaks for (110) and (101) after post-heating in air, orthorhombic Li₂MnSiO₄ (β -phase, space group *Pmn2₁*) was clearly formed.

The lattice parameter [$a = 6.3113\text{\AA}$, $b = 5.3805\text{\AA}$, and $c = 4.9924\text{\AA}$] of β -Li₂MnSiO₄ material was calculated by Rietveld refinement analysis and are consistent with values published by others [10,11].

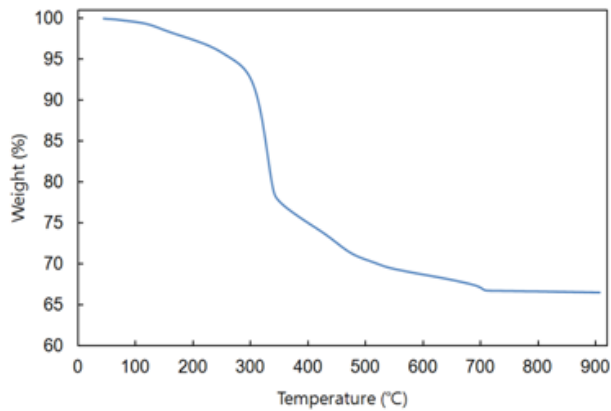


Figure 1. Thermogravimetric analysis of the mixture of precursors under N₂ atmosphere.

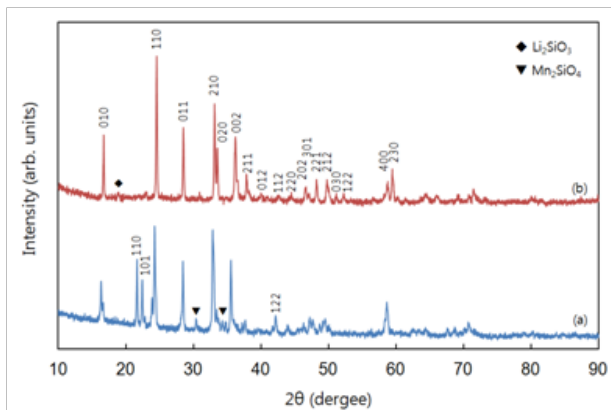
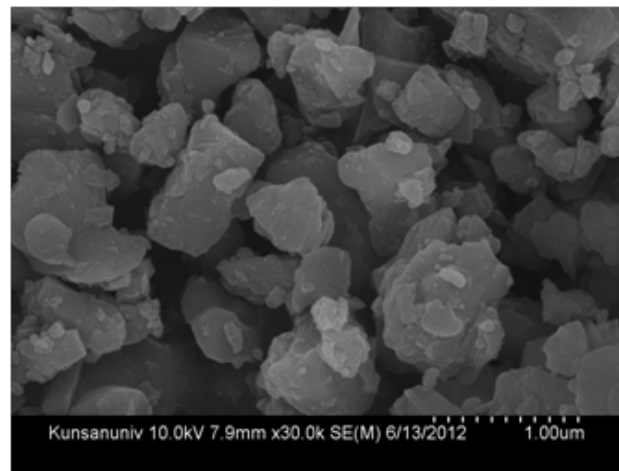


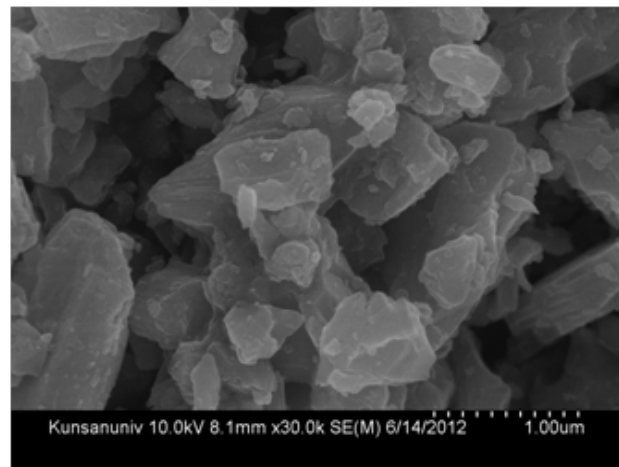
Figure 2. XRD patterns of Li₂MnSiO₄ sintered (a) at 900°C in N₂ for 12h and post-heated (b) at 400°C in air for 5h after sintering.

The change of morphology for the Li₂MnSiO₄ before and after post-heating was examined by FE-SEM and shown in **Figure 3**. Li₂MnSiO₄ does not have uniform size distribution with a particle diameter of approximately ~1 μ m containing nanosized particles (~100nm). A dramatic change of morphology after post-heating was not observed in **Figure 3(b)**. Bigger size particles (>1 μ m) are insufficiently conductive to allow for lithium ion diffusion and electric connection because very low conductivity of Li₂MnSiO₄. Therefore, carbon coating or incorporation should be considered the increase the electric conductivity and ion diffusivity [12]. EDS analysis was used to investigate a qualitative atomic composition and the results are shown in **Figure 4**. The content of Mn and Si is almost same and is not changed after post-heating.

Figure 5 shows the charge-discharge behaviors of synthesized two Li₂MnSiO₄ materials at room temperature. γ -Li₂MnSiO₄ had ~3mAh/g of discharge capacity, even though its theoretical capacity is 333mAh/g as 2 moles of Li⁺ are extracted from formula unit. The discharge capacity was increased dramatically changing crystal structure from γ -phase to β -phase. β -Li₂MnSiO₄ shows ~45mAh/g of discharge capacity



(a)



(b)

Figure 3. SEM images of Li₂MnSiO₄ (a) before and (b) after post-heating at 400°C.

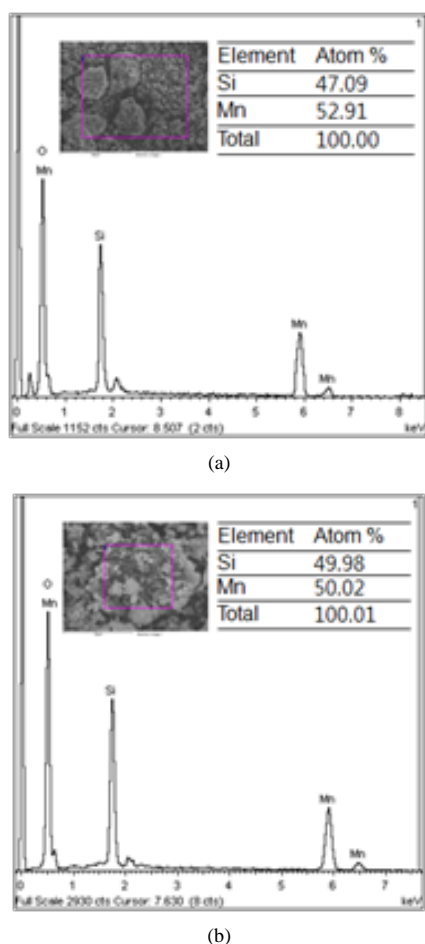


Figure 4. EDS analysis of $\text{Li}_2\text{MnSiO}_4$ (a) before and (b) after post-heating at 400°C .

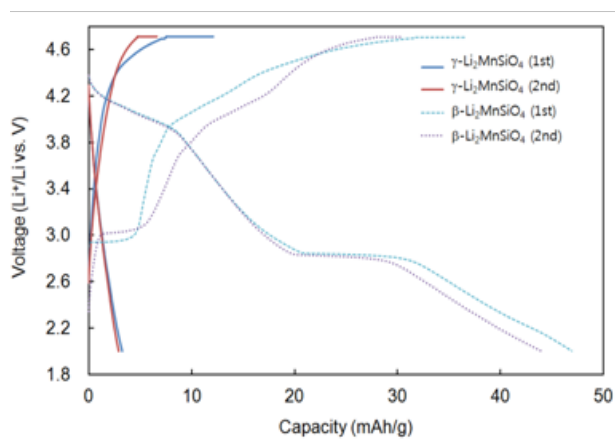


Figure 5. Charge-discharge curves of $\gamma\text{-Li}_2\text{MnSiO}_4$ synthesized at 900°C , and $\beta\text{-Li}_2\text{MnSiO}_4$ post-heated at 400°C after 900°C sintering.

which is 15 times higher than $\gamma\text{-Li}_2\text{MnSiO}_4$. Very low capacities of two materials are attributed to extremely low electric conductivity of $\text{Li}_2\text{MnSiO}_4$ ($3 \times 10^{-14} \text{ Scm}^{-1}$) [13]. To increase the electric conductivity of active material, carbon was coated on the surface conventionally. However, several studies re-

ported that uncoated $\text{Li}_2\text{MnSiO}_4$ usually had very low capacity [14,15].

In the charge-discharge profiles of two materials, $\beta\text{-Li}_2\text{MnSiO}_4$ has two plateaus during cycling, but $\gamma\text{-Li}_2\text{MnSiO}_4$ does not. dQ/dV plots of $\beta\text{-Li}_2\text{MnSiO}_4$ was shown in Figure 6 to identify the potentials of plateaus. The peaks may correspond to the voltages plateaus of the $\text{Mn}^{2+/3+}$ and $\text{Mn}^{3+/4+}$ redox couples. $\beta\text{-Li}_2\text{MnSiO}_4$ shows one sharp cathodic peak at $\sim 2.9\text{V}$, and two small peaks at ~ 4.0 and $\sim 4.1\text{V}$ during first charge. In contrast, $\gamma\text{-Li}_2\text{MnSiO}_4$ does not show any peak during both charging and discharging (not shown). At second cycle, the cathodic sharp peak moved from $\sim 2.9\text{V}$ to 3.0V , but the anodic peak did not. Arroyo-de Dompablo et al. calculated average lithium extraction voltage from Li_2MSiO_4 ($M = \text{Mn, Fe, Co}$ and Ni) [16]. They observed that in all cases extraction of the second lithium ion may occur at very high voltage ($>4.5\text{V}$) except for $\text{Li}_2\text{MnSiO}_4$, existing the possibility of the decomposition of LiPF_6 based electrolyte. But, by their calculation, the first and second lithium ion extraction from $\text{Li}_2\text{MnSiO}_4$ occurred at 4.1 and 4.5V , respectively. Muraliganth et al. reported $\text{Li}_2\text{MnSiO}_4$ showed a single cathodic peak at $\sim 4\text{V}$ and broad anodic peak at $\sim 3\text{V}$ at first cycle [17]. However, it did not exhibit a sharp peak at second cycle, assuming structural rearrangement and conversion of the crystal structure into an amorphous phase during the first charge. Similar behavior was observed in the results of Yang's group [11]. They reported that no strong peaks from XRD results could be observed when the electrodes were discharged below 3.2V . Unlike their results, our $\beta\text{-Li}_2\text{MnSiO}_4$ had clearly sharp peaks at second cycle because its structure still had crystallinity. However, we did not find any evidence or explanation for first peaks around $2.8\text{--}3.0\text{V}$ in our $\beta\text{-Li}_2\text{MnSiO}_4$, which was reported in many literatures. We are still trying to define for that. Conclusively, the lithium extraction from $\beta\text{-Li}_2\text{MnSiO}_4$ is more effective than that from $\gamma\text{-Li}_2\text{MnSiO}_4$. Politaev et al. reported that the two structure types differed in their mode of connecting tetrahedral and in connectivity of their rigid part, $(\text{MnSiO}_4)^{2-}$ [6]. The $\beta\text{-Li}_2\text{MnSiO}_4$ structure is layered (2D) whereas $\gamma\text{-Li}_2\text{MnSiO}_4$ structure is a framework (3D). They also described that the former had more freedom for Li^+ ion motion and, possibly, for Mn displacement into octahedral voids. In our work, the difference between two structures on electrochemical property may be attributed to same reason why they suggested.

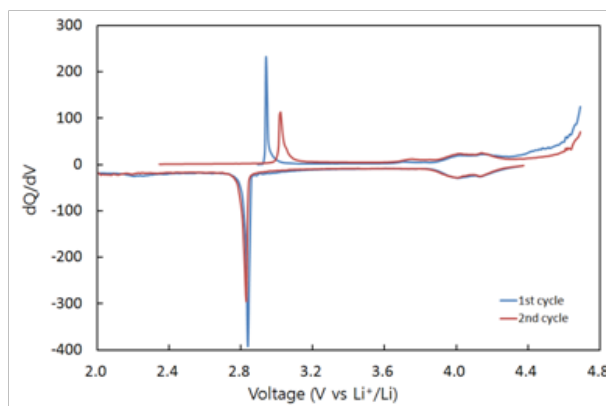


Figure 6. dQ/dV plots for charge-discharge curves of $\beta\text{-Li}_2\text{MnSiO}_4$.

4. Conclusions

A solid state reaction method has been used to synthesize $\text{Li}_2\text{MnSiO}_4$ with different crystal structure and with a minimal level of impurities. $\gamma\text{-Li}_2\text{MnSiO}_4$ has been produced by high temperature sintering at 900°C and then post-heating at 400°C changed its crystal structure from γ -phase to β -phase. In electrochemical measurement, two materials (γ - and β -phase) showed ~ 3 and $\sim 45\text{mAh/g}$, respectively. In the charge-discharge profiles of two materials, $\beta\text{-Li}_2\text{MnSiO}_4$ had two plateaus during cycling, but $\gamma\text{-Li}_2\text{MnSiO}_4$ did not. The difference between two materials on electrochemical property may be attributed to the crystal structure because β -phase had more freedom for Li^+ ion motion than γ -phase.

5. Acknowledgements

This work was supported by R&D Program through the National Fusion Research Institute of Korea (NFRI) funded by the government funds.

REFERENCES

- [1] W.-J. Zhang, *J. Power Sources* 196 (2011) 2962–2970.
- [2] M. S. Whittingham, *Chem. Rev.* 104 (2004) 4271–4301.
- [3] Z. Gong, Y. Yang, *Energy Environ. Sci.* 4 (2011) 3223–3242
- [4] T. Ohzuku, A. Ueda, *J. Electrochem. Soc.*, 141 (1994) 2972–2977.
- [5] R. Dominko, M. Bele, A. Kokalj, M. Gaberscek, J. Jamnik, *J. Power Sources*, 174 (2007) 457–461.
- [6] V.V. Politaev, A.A. Petrenko, V.B. Nalbandyan, B.S. Medvedev, E.S. Shvetsova, *J. Solid State Chem.* 180 (2007) 1045–1050
- [7] P. Tarte, R. Cahay, *C. R. Acad. Sci. Paris C* 271 (1970) 777.
- [8] M.E. Arroyo y de Dompablo, U. Amador, J.M. Gallardo-Amores, E. Moran, H. Ehrenberg, L. Dupont, R. Dominko, *J. Power Sources* 189 (2009) 638–642.
- [9] J. Kim, J. Shim, G. Park, H.-J. Sun, *J. Kor. Int. Electrical & Electronic Mater. Eng.* 25 (2012) 398–402
- [10] N. Kuganathan and M. S. Islam, *Chem. Mater.* 21 (2009) 5196–5202.
- [11] Y. X. Li, Z. L. Gong, Y. Yang, *J. Power Sources* 174 (2007) 528–532.
- [12] Z. Chen, J. R. Dahn, *J. Electrochem. Soc.* 149 (2002) A1184–A1189
- [13] A. Kokalj, R. Dominko, G. Mali, A. Meden, M. Gaberscek, and J. Jamnik, *Chem. Mater.*, 19 (2007) 3633.
- [14] I. Belharouak, A. Abouimrane, K. Amine, *J. Phys. Chem. C* 113 (2009) 20733–20737.
- [15] V. Aravindan, K. Karthikeyan, S. Amaresh, Y.S. Lee, *Electrochem. Solid-State Lett.* 14 (2011) A33–A35.
- [16] M.E. Arroyo-de Dompablo, M. Armand, J.M. Tarascon, U. Amador, *Electrochem. Comm.* 8 (2006) 1292–1298
- [17] T. Muraliganth, K. R. Stroukoff, and A. Manthiram, *Chem. Mater.* 22 (2010) 5754–5761